Morphology of Ge:Al thin films: Experiments and model

Yossi Lereah,[1] Irena Zarudi,[1] Enrique Grünbaum,[1] Guy Deutscher,[2]
Sergey V. Buldyrev,[3] and H. Eugene Stanley[3]
[1]*Faculty of Engineering, Tel Aviv University, Tel Aviv 69978, Israel*
[2]*Faculty of Exact Sciences, Tel Aviv University, Tel Aviv 69978, Israel*
[3]*Center for Polymer Studies and Department of Physics, Boston University, Boston, Massachusetts 02115*
(Received 30 December 1992; revised manuscript received 26 July 1993)

We report measurements on the branched morphology of the Ge core which grows inside the Al crystal during the crystallization of Ge:Al thin films. We quantitatively characterize this morphology by (i) two length scales $\lambda_\perp$ (the branch width) and $\lambda_\parallel$ (the branching distance) which are perpendicular and parallel to the growth direction and (ii) the typical angle θ between the branches. We find a qualitative similarity between films with various component concentrations and crystallization temperatures. However, these parameters influence the two length scales in a different fashion, thus influencing the angle between the branches. We further find that $\lambda_\perp \sim v^{-1/4}$, while $\lambda_\parallel$ depends more weakly on v ($\lambda_\parallel \sim v^{-1/6}$), where v is the growth velocity. Finally, we propose a model that combines features of the Eden model (for the growth of the Al crystal rim) and the diffusion-limited aggregation model (for the growth of the branched Ge fingers). The predictions of the model are compared with our experimental data.

PACS number(s): 68.70.+w, 68.35.Fx, 81.35.+k, 61.16.Bg

I. INTRODUCTION

A branched morphology which is unique in the field of materials science was discovered recently [1,2] as a part of a research project on the crystallization of amorphous Ge:Al thin films (see Fig. 1). These films afford a good opportunity to observe the crystallization process *in situ* by electron microscopy. Such observations supply information on two aspects: (i) the crystallization process which, due to its small velocity, can be followed even at high magnifications and (ii) branching morphology, which has been a subject of intense study in recent years. Most interestingly, the experimental system allows for direct study of the relationship between the microscopic process and the global morphology.

Experimental [2,3] and theoretical [4] studies reveal the following scenario for the creation of this unique morphology.

(i) Al crystals, tens of micrometers in diameter, spontaneously grow "colonies" in the Ge:Al amorphous phase matrix which contains a typical Ge concentration of 50%. The interface of the crystalline Al and the amorphous phase was examined by high-resolution electron microscopy and by electron nanoprobe x-ray analysis, and was reported to be fractal, with fractal dimension $d_f = 1.2$ [3]. The homogeneity of the concentration of Ge in the Al:Ge amorphous phase (even very close to the boundary with the Al rim) suggests that diffusion has no significant role in the growth of the Al crystalline phase. Accordingly, the Eden model may be relevant for characterizing the Al crystal growth. In qualitative agreement with expectation based upon the Eden model, "pockets" of amorphous phase are found in the crystalline Al matrix near the interface [3].

(ii) The Al crystal is saturated by Ge, the concentration of Ge near the boundary being $\approx 10\%$. However, the majority of the Ge is found as a crystalline core inside the Al crystal forming a dense (nonfractal) branched morphology (Fig. 1). The diffusion of Ge atoms from the amorphous phase into the Al rim is the key formation mechanism for this Ge core morphology. Experimental support for the idea that Ge diffuses in the Al crystalline phase was reported [1,2]. Specifically, we found the same temperature dependence for two quantities, growth velocity and ratio D/ξ (where D is the diffusion coefficient and ξ is the width of the Al "rim" surrounding the Ge "core").

(iii) We found the Ge core to be polycrystalline, indicating that nucleation of new Ge crystals occurs during its growth. The measurable parameter "nucleation rate" of the Ge crystals replaces [1,2] the parameter "reaction rate," which was introduced to describe the Ge growth probability [4]. The Al crystal and the Ge core grow at constant velocity v with constant rim width ξ. The growth of both Al crystal and Ge core is coupled: the amorphous phase contains typically 50% Ge, while the Al crystal only 10%, so the saturated Al cannot grow further unless the excess Ge diffuses and sticks to the Ge core. On the other hand, the branching of the Ge core enables part of it to be at constant distance from the amorphous phase; if the Ge core would grow as a compact object, then this distance would increase, and as the process depends on diffusion through this increasing gap, it would slow down.

In the field of pattern formation, two principal models are used to create aggregates: the Eden model, in which diffusion plays no role, and the diffusion-limited aggregation (DLA) model, in which diffusion is the determining feature [5]. The Eden aggregate is characterized as a compact cluster with a rough surface; the diffusion-controlled aggregate exhibits its characteristic branching. Both models have recently undergone intensive study, in

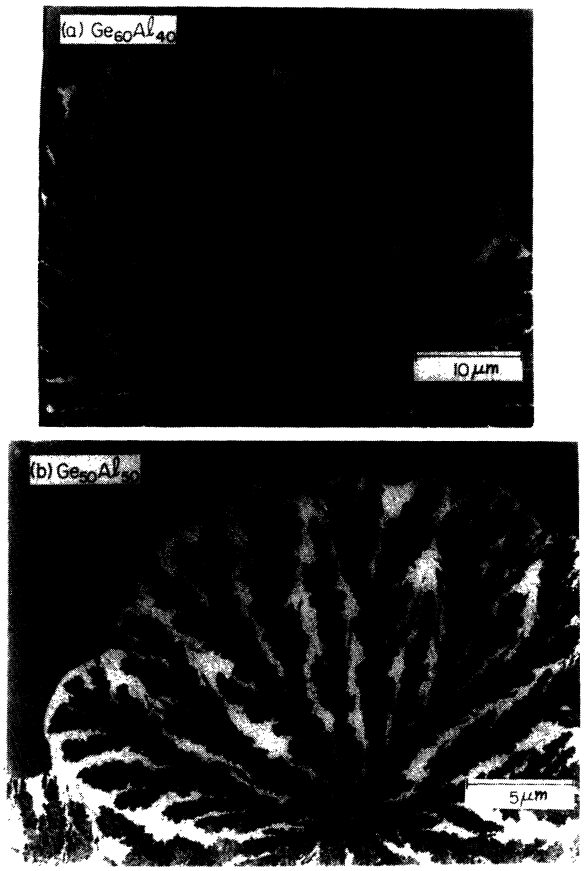

FIG. 1. Electron micrograph showing dense branching morphology of Ge_xAl_{1-x} alloys prepared with two different relative concentrations of Ge and Al: (a) $x = 0.6$ and (b) x=0.5. The resulting colony morphologies are qualitatively similar but differ in detail: in (a), there appear elongated branches without much branching, while in (b), the angles between the branches are larger and more branching occurs.

some modification of the principal rules governing their generation.

A classification of diffusion-controlled clusters in various systems was given in Fig. 1 of Ref. [6]. A number of systems (e.g., Hele-Shaw cell, electrodeposition, and crystallization of materials) reveal one of three types of branching morphology: fractal, dense, or isotropic. Recent studies on quantifying the DLA cluster anatomy have been carried out [7–9]. For example, the branch-length distribution was studied by Ossadnik [7] and Alstrøm [9]. Ossadnik [7] and Nittmann and Stanley [8] measured the average angle between DLA branches (and found 38° and 35°, respectively).

Following up on our previous studies [2,3] on Al:Ge thin films, we report here on the geometrical measurements which are obtained on the morphology of the branched Ge core that grows inside the Al crystal. These measurements supply a basis for quantitative comparison with branched morphologies in other systems. In particular, we introduce two characteristic lengths $\lambda_\perp$ and $\lambda_\parallel$, perpendicular and parallel to the growth direction. Unequal changes of these length scales arising from tuning experimental parameters (such as crystallization temperature or concentration of the two components) correspond to the underlying self-affinity of the problem. We shall discuss microscopic models that may be relevant to describing the experimental growth process and propose a specific lattice model that takes into consideration the characteristic features of the crystalline phase growth. The result of computer simulations of the model reveals a new generic shape that can be compared with the experimental results.

While an accurate analysis can be carried out for model systems, the analysis of experimental branched morphology is somewhat more difficult, because for typical experiments in the pattern formation field, the experimental clusters contain few orders of branching. However, the branched morphology in the present experimental study is of relatively high scale, i.e., each cluster contains hundreds of branching events thus supplying a sufficient basis for statistical studies. Furthermore, as the study is from materials science field, it is based on the well established techniques, which allow one to carry out well-controlled experiments.

II. EXPERIMENT

The method of preparation and the crystallization of the amorphous thin films of Ge:Al alloy is described in detail elsewhere [2], and we will give here only the most relevant information. Thin films of Ge_xAl_{1-x} ($0.45 < x < 0.60$) (of thickness ≈ 500Å) are prepared by coevaporation of the elements. After complete dissolution of the substrate, the films are mounted on electron microscope grids. Electron diffraction indicated that their structure is amorphous. The films are homogeneously heated with a special furnace in the electron microscope to a specific temperature in the range of 250–300° C, a temperature in which crystallization occurs. We performed crystallization of Ge-Al films with various element concentrations for a range of temperatures (held constant during the crystallization process). We find qualitatively similar dense branching morphologies, which differ from one another only in the quantitative details (Fig. 1).

In order to quantify the morphology, the following procedure is used (Fig. 2).

(i) The contours of the branches are plotted [Fig. 2(b)]. This stage sometimes requires judgement, since some branches recombine after growing independently for some distance. When this "recombination distance" is very short, a holelike structure is produced [Fig. 2(d)].

(ii) The central lines of the branches are drawn in this contour map, producing a "skeleton" [Fig. 2(c)] for which the following measurements are taken.

(a) The branch width $\lambda_\perp$, which is the characteristic length scale perpendicular to the growth direction, is measured by counting the number of branches of the skeleton which cross an imaginary line perpendicular to the growth direction.

(b) The distance $\lambda_\parallel$ between branches, a characteristic length scale parallel to the growth direction, is measured by counting the number of nodes (bifurcations) along the main branches.

(c) The angle θ between the branches is measured. We

find that many branches tend to bend after some distance toward the growth direction, so we measured the angles "locally" at the roots of the branches, and thereby obtained the distribution of angles between the branches.

From our transmission electron micrographs, all three measurements are made on samples having various concentrations. Each sample is crystallized at two distinct temperatures: one extremely low and the other extremely high. For some values of concentration, measurements are made at many different values of crystallization temperature.

Figure 3 shows the dependence of the two characteristic length scales $\lambda_\perp$ and $\lambda_\parallel$ on the growth velocity $v = dR/dt$ where R is the mean radius of the colony. Figure 4 shows the dependence of the angle θ between branches and the length scale ratio $\lambda_\perp/\lambda_\parallel$ as a function of concentration for low and high crystallization temperatures. We emphasize that the low and high crystallization temperatures are not identical for different concentrations, since the range of crystallization temperatures varies with concentration.

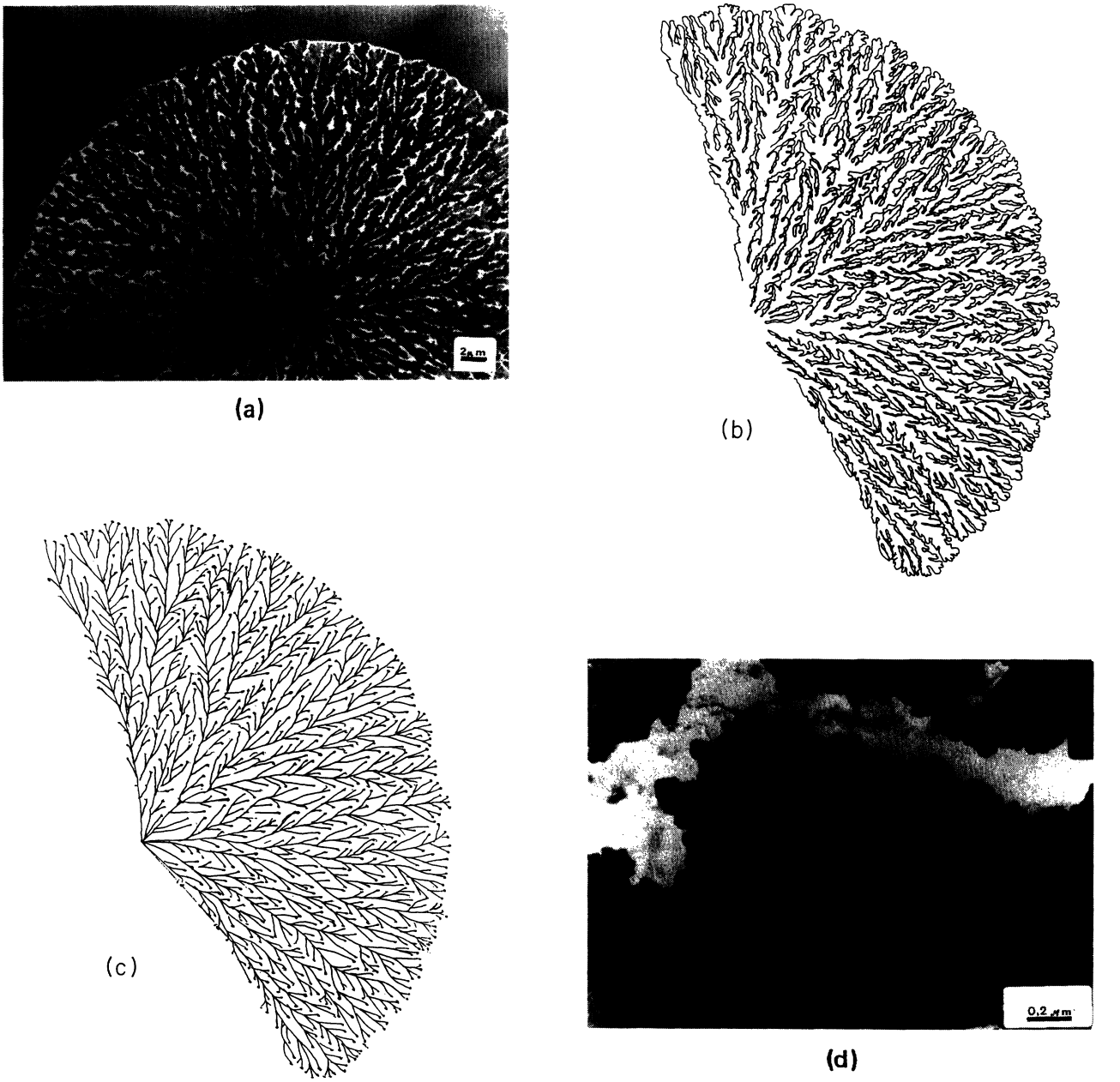

FIG. 2. The procedure of analyzing the length scales and angles between branches in the branched Ge core. (a) An electron micrograph of a representative colony studied in this work. (b) The contour scheme used for analyzing the branches in the colony. (c) The central lines in the contour creating the "skeleton" used in the present analysis. (d) A *high magnification* electron micrograph, demonstrating the difficulties in the determination of small branches due to confusion between branching events and holelike structure.

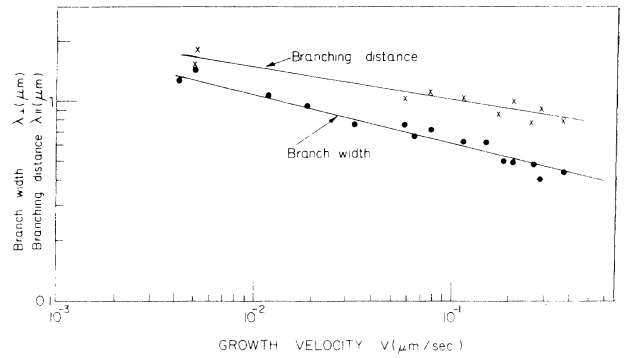

FIG. 3. Log-log plot showing the dependence of the two different characteristic length scales $\lambda_\perp$ and $\lambda_\parallel$ on growth velocity v. The slopes are, respectively, 1/4 and 1/6; note that the data points supporting slope 1/6 is fewer in number than supporting 1/4.

III. MODEL

The principal physical features of the growth mechanism, as discussed in the Introduction, are the following.

(i) Formation of Al crystal from the Ge:Al amorphous phase. No diffusion of Al takes places during its growth, thus suggesting that the Eden model would be appropriate in describing the Al growth [3].

(ii) Formation of the Ge core inside the Al crystal. Ge atoms diffuse from the amorphous phase inside the Al crystal and stick to the Ge core [2].

(iii) Coupling of the Al and Ge growth. The saturated Al crystal cannot grow further unless the excess of Ge has diffused and stuck to the Ge core.

In this section, we propose a model that incorporates features of the Eden model for growth of the Al crystal and of DLA for growth of the fingers comprising the Ge core. A computer simulation is devised to demonstrate the above processes and to test the model.

The model is defined as follows.

(i) To simulate the amorphous phase, a random distribution of Ge and Al is created by assigning the pixels of a square lattice to be Ge with probability p and Al with probability $1-p$.

(ii) An Al interface is advanced into the amorphous phase according to the Eden model with the following restrictions: if the interface advances into Al atom, then the Al atom becomes part of the Al crystal. However, if the Al interface advances into Ge atom, the Ge atom is released into the Al crystal and begins to undergo a lattice random walk confined to the Al crystal.

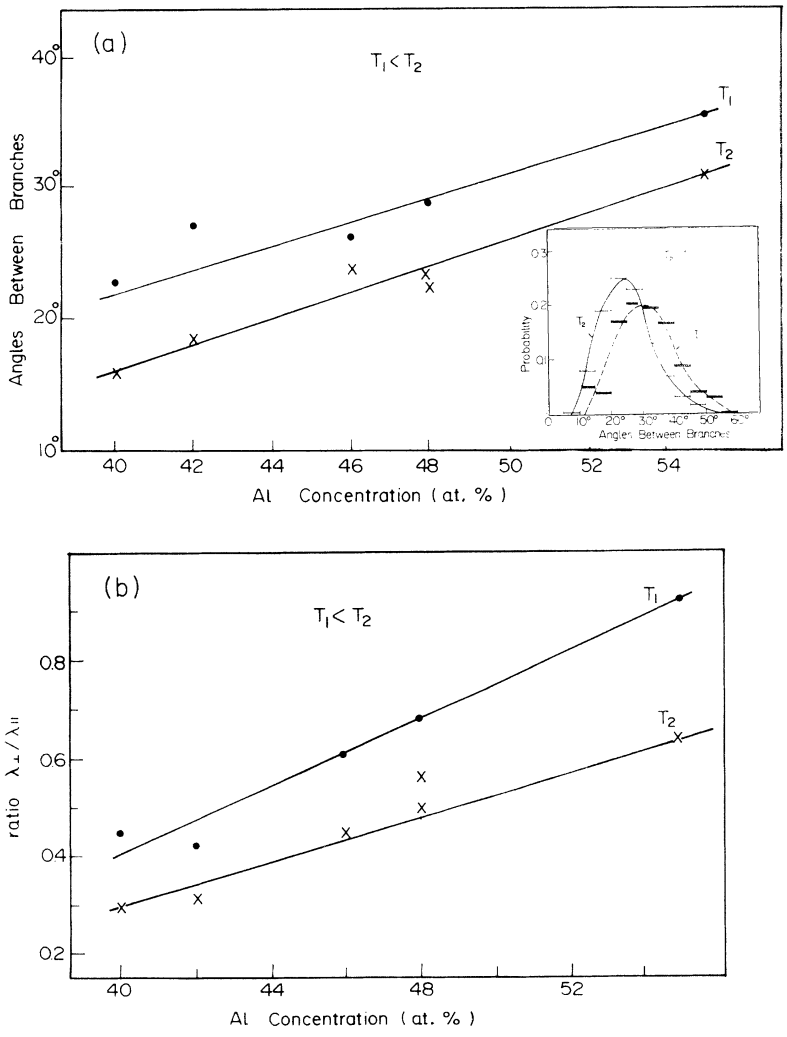

FIG. 4. (a) The dependence of the (most probable) angle θ between the branches on Al concentration for an extremely low crystallization temperature T_1 and an extremely high crystallization temperature T_2. Note that the branch angle increases with increasing Al concentration, with a maximum at roughly 35°, similar to the angle found for DLA [7–9]. Shown in the inset is the histogram of angles for the same two temperatures. (b) The dependence of the ratio $\lambda_\perp/\lambda_\parallel$ on Al concentration for the same two extreme values of crystallization temperatures.

(iii) The Ge atoms continue to diffuse in the Al crystal and irreversibly aggregate to form the Ge core, resulting in a fingerlike pattern.

(iv) At each unit of time, we move all Ge random walkers and attempt to move the interface at a randomly selected fraction p_i of the interface sites. The parameter p_i corresponds to the ratio between the growth velocity and the diffusion coefficient, since in one unit of time we move all Ge but only a fraction of the interface sites. Thus a small v/D ratio corresponds to a small value of the parameter p_i.

(v) The coupling of the Al and the Ge growth due to the limited solubility of Ge in the Al is simulated as follows. If the diffusing Ge atom hits the interface between crystalline Al and the amorphous phase, it is reflected and, moreover, the site on the interface which is hit becomes "frozen"—for each site on the interface, we calculate the number $K \equiv n_h - Rn_a$, where n_h counts the number of times this interface site is hit by Ge random walkers, n_a is the number of attempts to move the interface at this site, and R is a tunable parameter. If by the time of the current attempt $K \leq 0$, then the interface is advanced; otherwise, the value R is subtracted from K and the interface stays in place. This rule is designed to model the solubility of Ge in Al crystal. It can be justified as follows. In one unit of time, the probability that a site on the interface will be hit by a Ge random walker is $c_i/4$, where c_i is the concentration of Ge walkers occupying sites that are nearest neighbors of the interface. Thus in t units of time, $n_h = tc_i/4$. On the other hand, the number of attempts to move an interface is given by $n_a = tp_i$. The constraint $K = n_h - Rn_a \leq 0$ implies that $c_i \approx 4Rp_i$. Thus we relate the concentration of Ge near the interface to the parameters of the model.

(vi) The Ge nucleation rate is modeled as follows. When the Ge random walker hits the Ge aggregate it sticks with a sticking probability that depends on the curvature. If the local curvature is negative, then the sticking probability is given by the parameter p_s, while if the curvature is positive, then the sticking probability is set equal to ϵ, where $\epsilon \approx 0$. The curvature of the interface is calculated according to Viscek's algorithm [6,10] suitably modified to reduce artificial anisotropy and the relaxation of the aggregated particle is allowed to avoid porosity of Ge aggregate [10]. Since temperature influences diffusion rate and reaction rate differently, we can simulate the influence of temperature by keeping the diffusion rate constant [see rule (iv)] and changing the reaction rate (i.e., sticking coefficient p_s).

Figure 5 shows the results of simulations based upon the model. Qualitatively, the picture is in very good agreement with the results of experiment for corresponding Al concentrations. The absolute values of Al concentration for the aggregates of the same morphology differ from model and experiment: In the experiments the phases of Ge and Al crystals are not pure but contain some fraction of the other species. Notice that the Al rim follows the Ge fingers in such a way that the width of the Al rim, ξ, is time independent and the Al front is even locally coupled with the Ge core, exactly as observed experimentally (Fig. 1). Quantitative measurements of the branch geometry are made using an aggregate which started from a line (in order to minimize the effect of anisotropy). Figure 6 shows how concentration and the sticking coefficient affect the ratio of the two characteristic length scales $\lambda_\perp/\lambda_\parallel$ and an average angle θ between the branches. Similar to the experiment results, the ratio

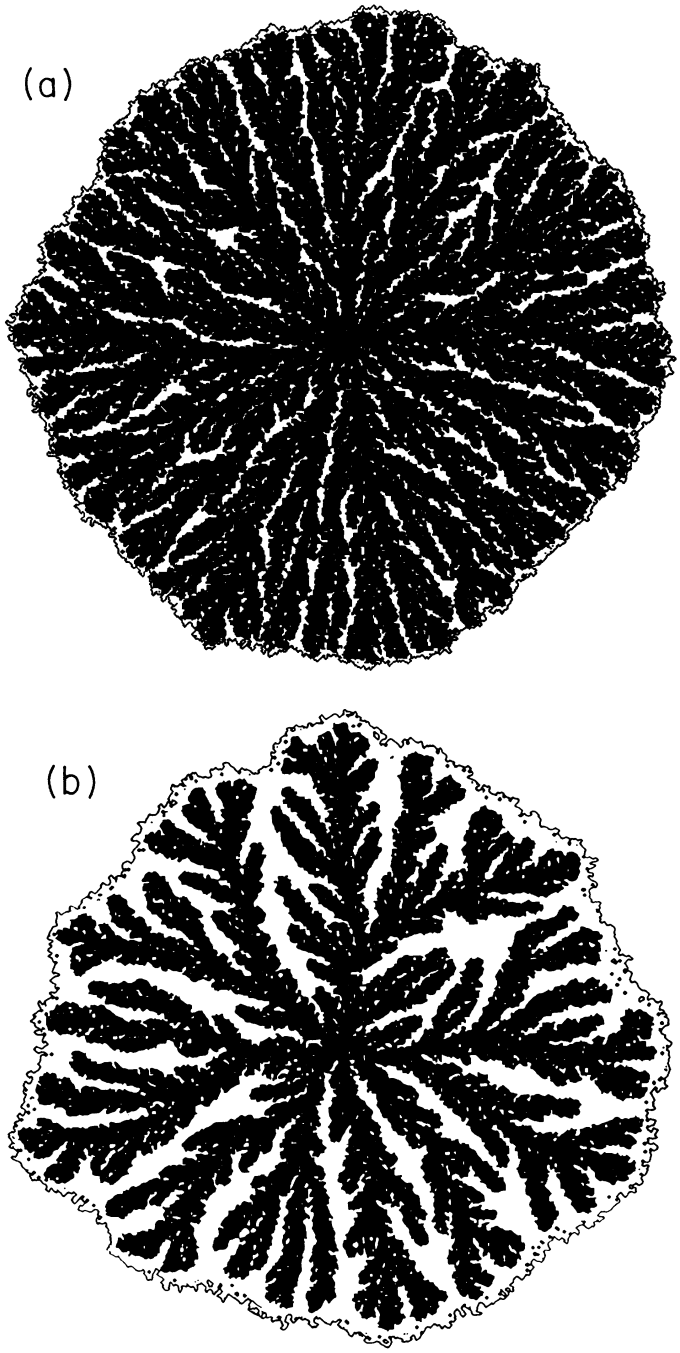

FIG. 5. Typical patterns generated by the model, using 16 000 particles in the colony. The Ge fingers are shown as black pixels and the Al crystal as white pixels. The rough interface separates the colony from the amorphous phase (a) $Al_{0.2}Ge_{0.8}$ and (b) $Al_{0.4}Ge_{0.6}$. The concentrations are chosen to correspond roughly to the experimental patterns shown in Fig. 1. Other parameters in the model are chosen as follows: $p_i = 0.0001, p_s = 1, R = 1$, and $\epsilon = 0.01$.

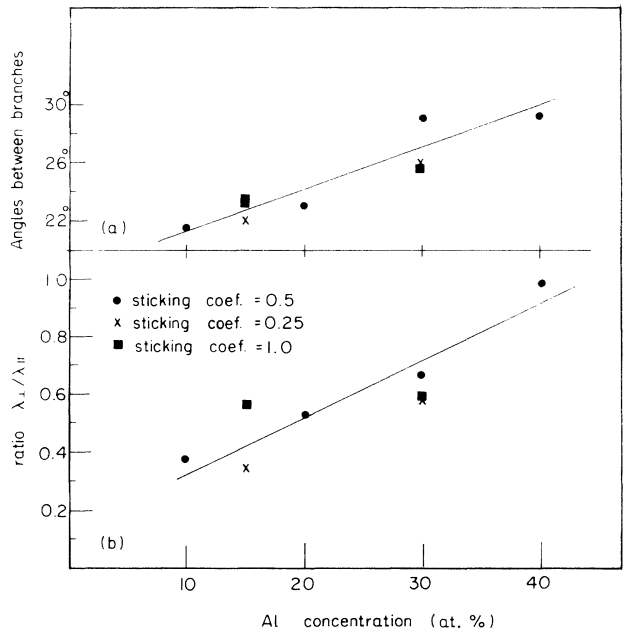

FIG. 6. The dependence predicted by the computer-simulated patterns of (a) the angles between the branches and (b) the ratio $\lambda_\perp/\lambda_\parallel$ on Al concentration for different sticking probabilities.

$\lambda_\perp/\lambda_\parallel$ and the angle θ increase with the Al concentration. However, the sticking coefficient does not influence these parameters in any systematic way.

We perform a systematic study of how the growth velocity v, the width of the aluminum rim ξ, and the average width of the branch $\lambda_\perp$ depend on the sticking probability p_s. As expected, we find that $\lambda_\perp$ and ξ decrease and v increases with the increase of p_s. We find that $v \sim 1/\xi \sim \lambda_\perp^{-d}$, as it should be according to the diffusion mechanism of the growth of Ge aggregate. On the other hand, we find that $v \sim p_s^{0.45\pm0.1}$. This exponent value is within experimental error of 0.5, which is predicted theoretically in [4] for the dependence of v upon the reaction rate (which in turn is modeled by the sticking probability). However, $\lambda_\perp$ appears to be proportional to ξ for a wide range of other parameters; this result is different from theoretical predictions and not consistent with the results of the experiment, possible due to the fact that the model in its present stage does not incorporate the polycrystalline structure of the Ge aggregate (see discussion below).

IV. DISCUSSION

A. Nonfractality of the Ge core

The nonfractal two-dimensional nature of the branched Ge is already reported [11]. However, it is not completely understood (see, e.g., Ref. [6], p. 322). The computer simulations clearly demonstrate the physical reason for it. As the Al crystal grows according to the Eden model, it creates a two-dimensional space in which the Ge precipitates to form the branched core. As the Ge concentration is well defined by that of the initial amorphous phase, this concentration has to be preserved in the final structure after the crystallization process, independent of distance from the center, thus creating a nonfractal object. The creation of the narrow Al rim which determines a diffusion length is an outcome of the described inputs into the computer simulations. This is contrary to the Smith-Collins simulations [12]. In their simulations the finite diffusion length is artificially introduced, resulting in two-dimensional branched aggregate.

B. Influence of concentration on characteristic length and angle

We obtained quantitative comparison between the branched Ge in the experiments and in the simulation by comparing the length scales of the branches and the influence of different parameters on them. In both systems it is difficult to determine branch width and branching distance for the following reasons.

(i) The branching is not always unambiguously defined, since occasionally recombination occurs leaving a structure with "holes" (see Figs. 1, 2, and 5).

(ii) The branches are rough and nonuniform in width. It is frequently difficult to determine whether a given part of a configuration is a single wide branch or two parallel narrow ones.

Nevertheless, these confusions do not obscure our immediate impression of the length scales and allow a visual qualitative comparison between pictures with different length scale (see [13] and Fig. 1). Two experimental parameters are found to influence the characteristic length scales $\lambda_\perp$ and $\lambda_\parallel$: (i) the Al and Ge initial concentrations and (ii) the crystallization temperature. Experimentally it is impossible to isolate the influence of each parameter as they are well correlated: the higher is the Al concentration in the amorphous phase the lower is the range of crystallization temperatures. Due to the different influence of both parameters (concentration and crystallization temperature) on both characteristic length scales, we find that a best basis for comparison is the ratio of the two length scales $\lambda_\perp/\lambda_\parallel$ and the angle between the branches θ. These characteristics supply information on the shape of the branched Ge irrespective of any scaling effect of the above parameters.

The experimental results (Figs. 3 and 4) show that the branched Ge should be regarded as self-affine objects. When samples of different component concentration crystallize, differences in the $\lambda_\perp/\lambda_\parallel$ ratio and in angles between the branches θ are revealed. The lower the Ge concentration, the higher the $\lambda_\perp/\lambda_\parallel$ ratio, and the higher the angle between the branches θ.

It is interesting to note that the maximum angle which is found is 35°, similar to that found in computer simulations of DLA [7–9] for aggregates with no restriction of concentration. The computer simulations give similar dependence of $\lambda_\perp/\lambda_\parallel$ and θ on concentration (Fig. 6). Thus, it is concluded that this effect is due to a general geometrical consideration which is included in the simulation. The possibility that this effect is caused by a metallurgical consideration (e.g., local anisotropy due to

crystalline structure) is excluded. We assume that the dependence results from a dynamical geometrical consideration, such as anisotropy in the flux of Ge particles. This consideration is being studied now by video observation of the process. The agreement of the computer simulation results with the experimental ones suggests that dynamical simulations should be studied alongside of videotaped records of the experimental work.

C. Influence of temperature

While the influence of concentration on the shape of the branched Ge (the ratio $\lambda/\lambda_{\|}$ and θ) is clearly seen (Fig. 1), we find the influence of the crystallization temperature on these parameters only after we take careful quantitative measurements (Fig. 4). The effect of temperature is introduced into the simulation by changing the Ge sticking coefficient. It was first suggested by Alexander *et al.* [4] that this parameter is equivalent to Ge reaction rate. Thus, if temperature influences diffusion and reaction rate differently, keeping one of them (diffusion) constant (using the computer clock), the changing of the other (reaction rate, i.e., sticking probability) will take the role of changing temperature. Although, the sticking probability influences the length scales (the lower the sticking probability the higher the length scales, in agreement with experimental results) no evidence is found in the computer simulations that this parameter influences the two length scales differently, i.e., that the ratio $\lambda_{\perp}/\lambda_{\|}$ changes. Also, no evidence is found that the sticking probability influences the angle between branches (Fig. 6).

We therefore suggest that the experimental observation—that the ratio $\lambda_{\perp}/\lambda_{\|}$ and the angle θ depend on crystallization temperature—originates in the specifics of the metallurgical system. The following should be considered: One additional influence of crystallization temperature on the system is the solubility of Ge in the Al crystal. Samples that contain 50% Ge in the amorphous phase when crystallized at the lowest crystallization temperature ($\approx$250° C) revealed $\approx$10% of Ge in the Al crystals near their rim, as is indicated by electron microprobe x-ray analysis. This high concentration (high compared to the expected one according to the standard phase diagram) is explained [4] by an extension of the solidus line below the eutectic temperature. According to this concept it is expected that at higher crystallization temperature this concentration will be lower.

The suggested decrease of Ge concentration in the Al rim with increasing temperature can be determined directly by x-ray analysis using an electron nanoprobe, which is required because of the small width of the rim at high temperature. For lack of present availability of this nanoprobe, we use an alternative method based on the determination of the concentration change with temperature of the Al phase in the region of the Ge core. This assumes that the atomic concentration of this phase does not change with temperature. The pictures of the branched Ge core were digitized and the ratio of the Al phase area to that of the Ge phase area was measured for samples of different nominal concentration which were prepared at two different temperatures T_1 and T_2, for each concentration value (Fig. 7). It is seen that the higher the crystallization temperature, the lower is the Al phase concentration.

We suggest therefore that the experimentally observed influence of the temperature on the ratio $\lambda_{\perp}/\lambda_{\|}$ and on the angle θ is related to the Al concentration, which has been shown both experimentally and by simulation to influence these two values (Fig. 6).

D. Connection between characteristic length and growth velocity

An important factor determining the length scale in the branched Ge core is the nucleation rate N of new Ge crystals during the growth. Since the total amount of Ge is fixed, the larger is the number of crystals the smaller they must be. We observed that the branch width $\lambda_{\perp}$ is comparable in size to the largest Ge crystals [2].

The relation between growth velocity v and nucleation rate N is [4]

$$v \sim (DN)^{1/2}, \tag{4.1}$$

where N is the number of nucleation events of Ge crystals per unit time and per unit length of the advancing Ge front. On the other hand, v must be proportional to the number of nucleation events times the average volume of the Ge crystal. If the linear dimension characterizing the Ge crystallites is assumed to scale as $\lambda_{\perp}$, then

$$v \sim N\lambda_{\perp}^{d}, \tag{4.2}$$

where d is the effective dimension of the Ge crystals. From Eqs. (4.1) and (4.2), it follows that

$$\lambda_{\perp} \sim (D/N)^{1/2d}. \tag{4.3}$$

We find experimentally that both D and v have charac-

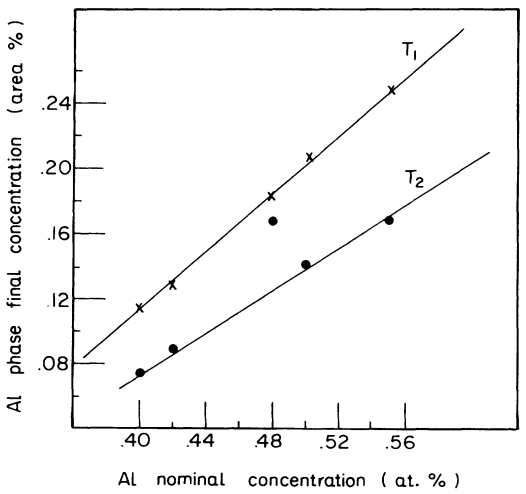

FIG. 7. The dependence of the Al phase concentration in the crystallized colony on the nominal concentration, i.e., on the Al atomic concentration in the amorphous phase, for the same two extreme values of crystallization temperature T_1 and T_2 of Fig. 4.

teristic Arrhenius temperature dependences. According to [14],

$$D \sim \exp(-1.2/kT), \tag{4.4a}$$

while from [1]

$$v \sim \exp(-3.6/kT), \tag{4.4b}$$

where $k = 0.86 \times 10^{-5}$ eV/K is the Boltzmann constant. Hence from Eq. (4.1), we expect

$$N \sim \exp(-6/kT). \tag{4.4c}$$

Taking into consideration experimental relations (4.4), one can derive from Eq. (4.3) that

$$\lambda_{\perp} \sim \exp(1.2/kT) \quad (d = 2) \tag{4.5a}$$

and

$$\lambda_{\perp} \sim \exp(0.8/kT) \quad (d = 3). \tag{4.5b}$$

On the other hand, from Fig. 3 it follows that

$$\lambda_{\perp} \sim v^{-1/4} \sim \exp(0.9/kT). \tag{4.5c}$$

Hence we conclude that the effective dimension d is between 2 and 3. This is consistent with the fact that the film thickness is 500 Å, which is 5–10 times the smallest crystals whose nucleation rate determines the velocity, while this thickness is 10–20 times smaller than the large crystals that determine the branch width $\lambda_{\perp}$. The exact reason for correlation between the branch width and the largest Ge crystals is not well understood and is under intensive study using video records of the branching phenomenon.

Since the width ξ of the Al rim is given by D/v [1], one can derive from Eqs. (4.1) and (4.2) that $\xi \propto \lambda_{\perp}^{d}$, which is not consistent with the results of computer simulations—perhaps because the model does not take into account the crystallite structure of the Ge core and the film thickness.

V. CONCLUSIONS

We have carried out quantitative measurements of dense branching morphology in the Ge:Al system. Our measurements include two characteristic length scales as well as the angles between branches. We find that these quantities depend on the concentration of Al and Ge, as well as on the crystallization temperature. We also propose a stochastic model which combines features of the Eden model and the DLA model. The results are in good agreement with the experiments and demonstrate well the dense nature of the branched aggregate.

We quantify the simulated branched aggregate (in a way similar to that of the experimental one) for various component concentrations and for various sticking probabilities in order to simulate various crystallization temperatures. We also find that (a) the dependence of concentration on the parameters of the model is in agreement with experiment, and (b) the influence of the sticking probability in the simulations differs from the experiment. We find that the branch width depends upon the growth velocity as $v^{-1/4}$ and interpret this result in terms of the nucleation rate of Ge crystals. Finally, we find that the influence of the sticking probability in the model differs from that of crystallization temperature in the experiments and resolve this apparent discrepancy by metallurgical considerations.

ACKNOWLEDGMENTS

We want to thank P. Alstrøm and A.-L. Barabasi for useful discussions, and S. Havlin, P. Ossadnik, and S. Schwarzer for helpful comments on the manuscript. This work is supported by the U.S.–Israel Binational Science Foundation under Grant No. 89-00459 and by the Israeli Ministry of Science and Technology.

[1] G. Deutscher and Y. Lereah, Phys. Rev. Lett. **60**, 1510 (1988).
[2] Y. Lereah, G. Deutscher, and E. Grunbaum, Phys. Rev. A **44**, 8316 (1991).
[3] Y. Lereah, J. M. Penisson, and A. Bourret, Appl. Phys. Lett. **60**, 1682 (1992).
[4] S. Alexander, R. Bruinsma, R. Hilfer, G. Deutscher, and Y. Lereah, Phys. Rev. Lett. **60**, 1514 (1988).
[5] *Fractals and Disordered Systems*, edited by A. Bunde and S. Havlin (Springer-Verlag, Heidelberg, 1991); *On Clusters and Clustering: From Atoms to Fractals*, edited by P. J. Reynolds (North-Holland, Amsterdam, 1993); H. J. Herrmann, Phys. Rep. **136**, 153 (1986); in *On Growth and Form*, edited by H. E. Stanley and N. Ostrowsky (Martinus Nijhoff Publishers, Dordrecht, 1986).
[6] T. Vicsek, *Fractal Growth Phenomena*, 2nd ed. (World Scientific, Singapore, 1992).
[7] P. Ossadnik, Phys. Rev. A **45**, 1058 (1992).
[8] J. Nittmann and H. E. Stanley (unpublished); see also Nature 321, 663 (1986).
[9] P. Alstrøm, in *Random Fluctuations and Pattern Growth: Experiments and Models*, edited by H.E. Stanley and N. Ostrowsky (Kluwer Academic Publishers, Dordrecht, 1988), p. 340.
[10] T. Vicsek, Phys. Rev. A **32**, 3084 (1985); Phys. Rev. Lett. **53**, 2281 (1984).
[11] E. Ben-Jacob, G. Deutscher, P. Garik, N. D. Goldenfeld, and Y. Lereah, Phys. Rev. Lett. **57**, 1903 (1986).
[12] R. L. Smith and S. D. Collins, Phys. Rev. A **39**, 5409 (1989).
[13] Y. Lereah, in *Random Fluctuations and Pattern Growth: Experiments and Models* (Ref. [9]), p. 125; G. Deutscher and Y. Lereah, Physica **140A**, 191 (1986).
[14] N. L. Peterson and S. J. Rothman, Phys. Rev. B **1**, 3264 (1970).

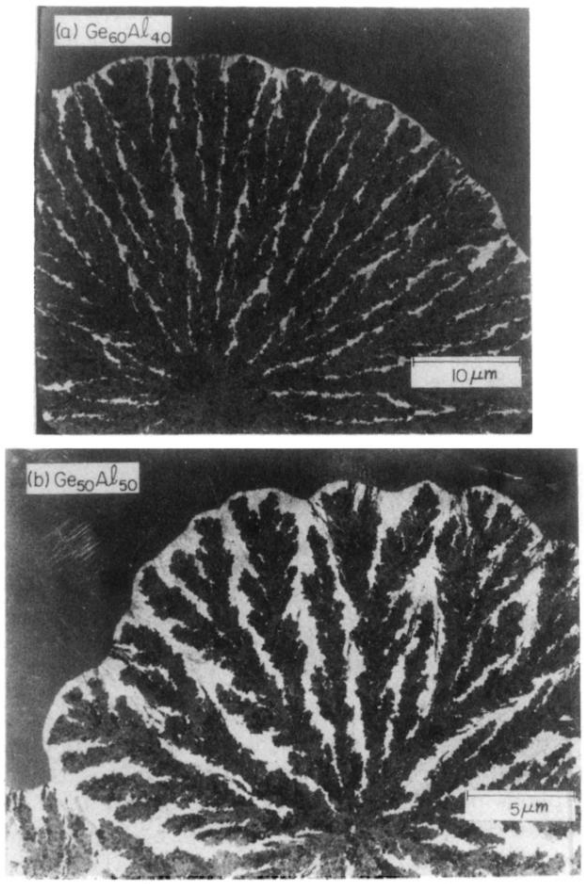

FIG. 1. Electron micrograph showing dense branching morphology of Ge_xAl_{1-x} alloys prepared with two different relative concentrations of Ge and Al: (a) $x = 0.6$ and (b) x=0.5. The resulting colony morphologies are qualitatively similar but differ in detail: in (a), there appear elongated branches without much branching, while in (b), the angles between the branches are larger and more branching occurs.

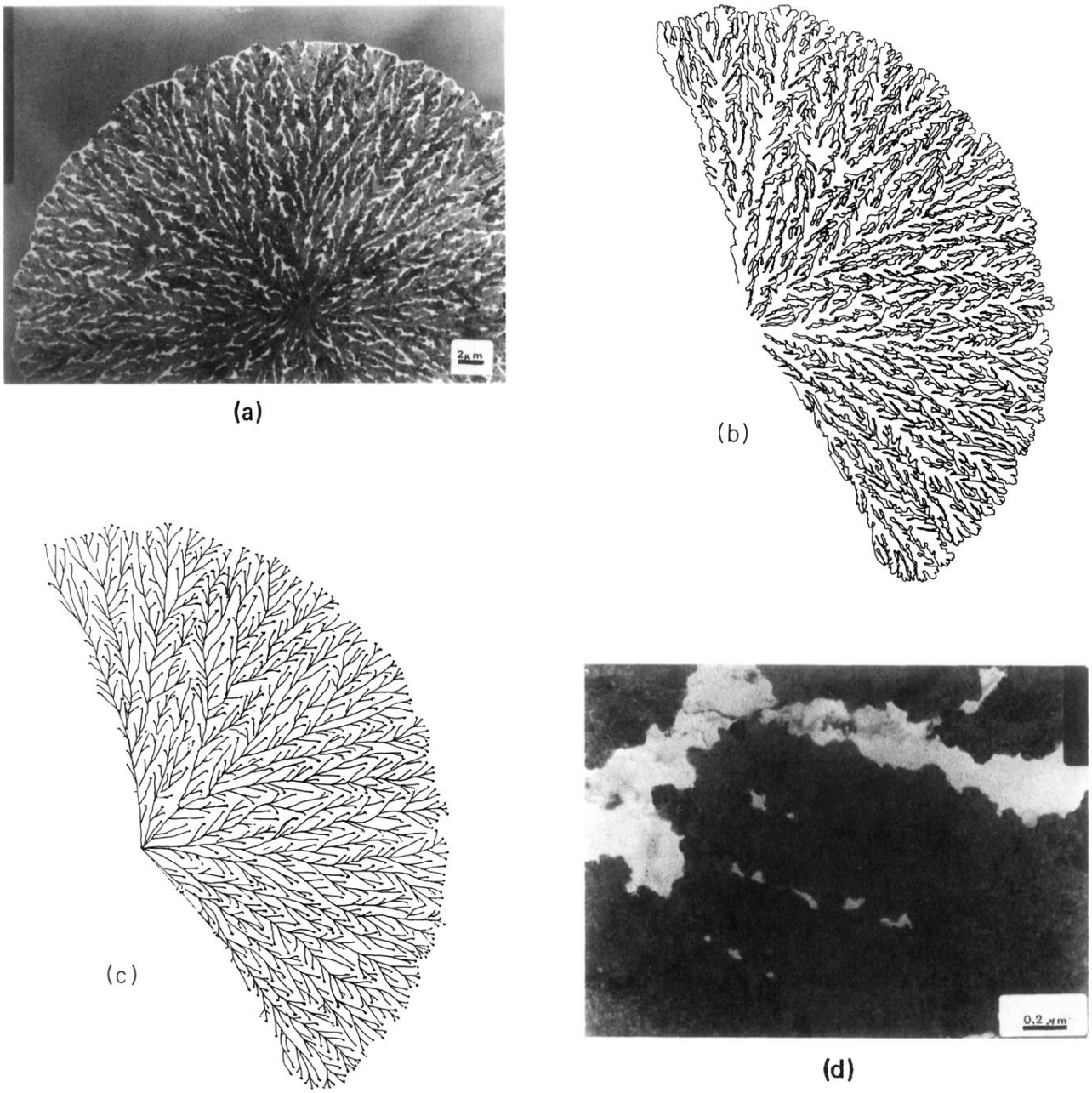

FIG. 2. The procedure of analyzing the length scales and angles between branches in the branched Ge core. (a) An electron micrograph of a representative colony studied in this work. (b) The contour scheme used for analyzing the branches in the colony. (c) The central lines in the contour creating the "skeleton" used in the present analysis. (d) A *high magnification* electron micrograph, demonstrating the difficulties in the determination of small branches due to confusion between branching events and holelike structure.

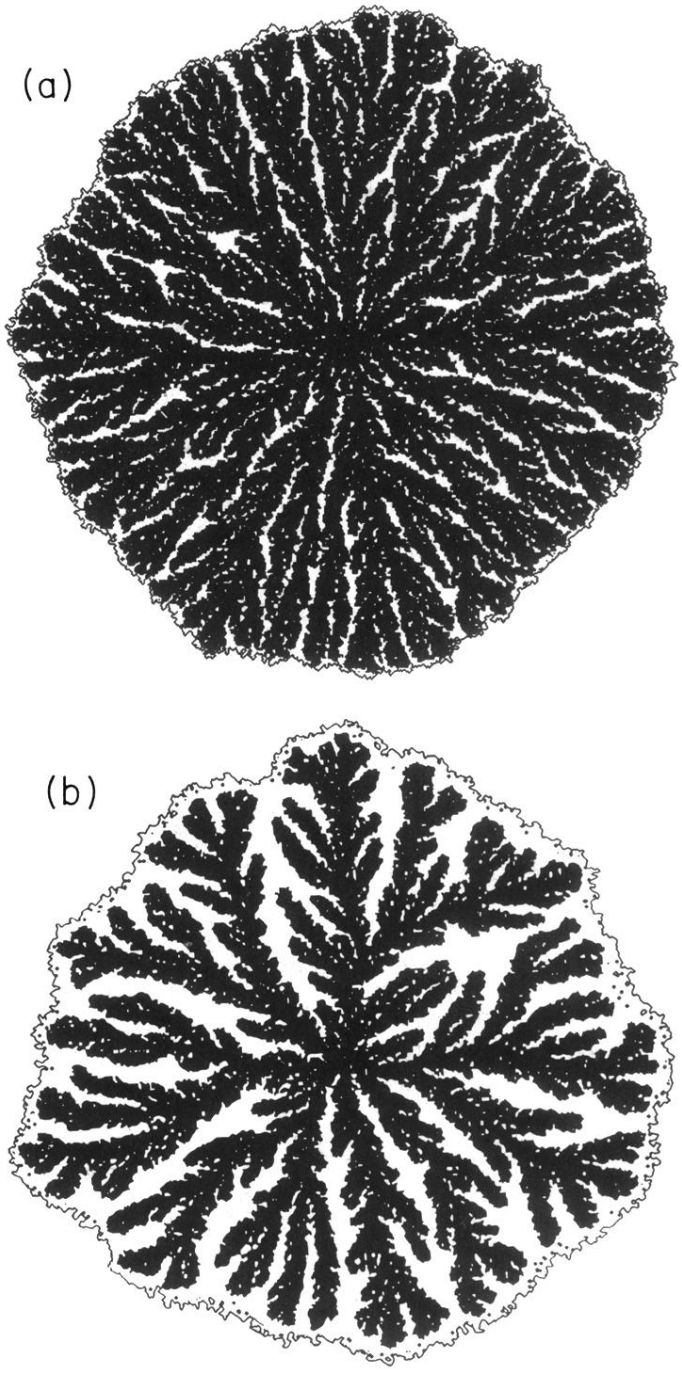

FIG. 5. Typical patterns generated by the model, using 16 000 particles in the colony. The Ge fingers are shown as black pixels and the Al crystal as white pixels. The rough interface separates the colony from the amorphous phase (a) $Al_{0.2}Ge_{0.8}$ and (b) $Al_{0.4}Ge_{0.6}$. The concentrations are chosen to correspond roughly to the experimental patterns shown in Fig. 1. Other parameters in the model are chosen as follows: $p_i = 0.0001, p_s = 1, R = 1$, and $\epsilon = 0.01$.